Journal of Materials Chemistry

Cite this: J. Mater. Chem., 2011, 21, 9576

www.rsc.org/materials

PAPER

Light transmission from the large-area highly ordered epoxy conical pillar arrays and application to GaN-based light emitting diodes

Xing-Xing Fu,[a] Xiang-Ning Kang,*[a] Bei Zhang,[a] Chang Xiong,[a] Xian-Zhe Jiang,[a] Dong-Sheng Xu,[b] Wei-Min Du[a] and Guo-Yi Zhang[a]

Received 9th March 2011, Accepted 12th April 2011
DOI: 10.1039/c1jm11027f

To improve the light transmission from the surface, we report a facile and cost-effective approach for the formation of wavelength-scale conical pillar arrays on a large surface area of epoxy resin. The highly ordered epoxy conical pillar arrays with a pitch of about 460 nm and height of about 800 nm have been successfully fabricated by the technique of shape-controlled anodization of Al foil followed by hot embossing. By replicating the tapered pore arrays onto a transparent semi-cylindrical epoxy structure, the incident angular resolved light transmission of the epoxy conical pillar arrays has been obtained. The integrated transmission of conical pillar arrays as high as 62.2% has been achieved which is confirmed to be 223% and 11.3% higher than that of planar epoxy and the cylindrical pillar arrays, respectively. It is reasonable to consider the wavelength-scale conical pillar array as a particular multilayer consisting of a series of two-dimensional photonic crystals with gradually increasing filling factor towards the surface. It can therefore be treated as a multilayer with continuously reducing refractive index towards the air. The conical and cylindrical pillar arrays of epoxy have been directly employed as the encapsulant of a GaN based flip-chip LED. Compared to the LED encapsulated by planar epoxy, the enhancement of light extraction from the LED covered with conical and cylindrical pillar arrays have been demonstrated to be 46.8% and 34.9%, respectively.

1 Introduction

One of the fundamental problems and challenges in solid state lighting is the small extraction efficiency for spontaneous emission resulting from the high refractive index contrast between the active material and the air.[1–6] For example, most light emitted from the planar surface of a GaN based light emitting diode (LED) is trapped inside the device due to total internal reflection (TIR) occurring at the boundary between the GaN layer and the air, and only about 4% of light can escape to the air.[3] Moreover, even for the encapsulated domes of the package, the loss from Fresnel reflection could still occur. To extract the trapped optical modes from the LED, there has been a great deal of research interest in introducing photonic crystals (PhC),[5] or packaging by transmissive or antireflection (AR) surface structures.[2,6–9] The application of shallow etched PhC gratings has been intensively demonstrated to improve the light extraction by their diffraction effect.[10–12] From our previous work on PhC,[13–15] we have found that the lattice pitch of PhC around wavelength-scale to micron-scale is beneficial to the light extraction of GaN based LEDs. However, a commercial application of PhC will additionally depend on the properties of state-of-the-art devices. The PhC is mostly fabricated by electron-beam lithography (EBL),[10] holographic lithography,[11] and focused ion beam milling (FIBM),[12] *etc.* which are limited by expensive equipment and low yield for mass production, particularly limited for large-scale chip fabrication. So developing a cost-effective large-area template of PhC for application to GaN based LEDs is highly desirable.

Recently, the geometrical structures of porous anodic alumina (AAO) have been found to be suitable for the formation of large area two-dimensional PhCs (2D-PhCs) with high aspect ratio (the hole depth divided by its size).[16,17] Self-ordered AAO templates with the lattice pitch varying from 100 nm to 500 nm could be fabricated by adjusting the anodization voltages, temperature, the type and concentration of acidic electrolytes.[18] On the other hand, Kim *et al.*[19] proposed an effective light out-coupling method of employing multilayer graded-refraction-index (GRIN) micro-pillar arrays with a pitch of about 2–5 μm. They reported a complete elimination of the total internal reflection and about 73% enhancement of the light output. But the materials and the geometric conditions were critical in their method of sputtering or deposition. It is also worthy of note that the AR structures made by patterning the surface with two-dimensional pillar arrays, the so-called pyramid-shaped 'moth eye' structures,[20–25] are an attractive alternative to the

[a]*School of Physics and State Key Laboratory of Artificial Microstructure and Mesoscopic Physics, Peking University, Beijing, 100871, China. E-mail: xnkang@pku.edu.cn; Fax: +86-10-62751615; Tel: +86-10-62751739*
[b]*Institute of Physical Chemistry, Peking University, Beijing, 100871, China*

conventional thin film stack coating. By using AAO templates with highly ordered tapered pore arrays, T. Yanagishita *et al.*[24] and K. Choi *et al.*[25] reported the light transmission of the polymer surface patterned by the tapered holes was enhanced effectively compared to that of the smooth surface. Both of the lattice pitches they prepared were around 100 nm. However, considering the practical application of the GaN-based LED, a shallow PhC is usually acting as a two-dimensional diffraction grating.[5] The lattice pitch of the PhC should be larger than 100 nm to satisfy the Bragg diffraction condition for extracting trapped optical modes.[13,26] In this case, study of the two-dimensional conical pillar arrays with a pitch around wavelength-scale is an interesting topic.

Epoxy resin has been extensively used as an encapsulant of LEDs due to its good mechanical and optical transmission properties. Moreover, epoxy resin has an excellent fluidness which is feasible for reprinting and transferring sub-micron structures. So, the formation of sub-micron structures and encapsulation can be simultaneously obtained during the LED fabrication process.

In this paper, we report the preparation of highly ordered tapered pore arrays of AAO with a pitch of about 460 nm and depth of about 800 nm by the shape-controlled technique.[24] An AAO sample as large as two inches in diameter was fabricated successfully. The conical pillar arrays of epoxy resin were transferred by the hot embossing technique from the tapered pore arrays of AAO. The incident angular-resolved light transmission was investigated on a specially formed hemi-cylindrical epoxy sample with conical pillar arrays. The transmission improvement and the application of the conical and cylindrical pillar arrays of epoxy as the encapsulant on the GaN based flip-chip LED (FC LED) are presented.

2 Experimental section

Fabrication of high ordered porous anodic aluminum templates

AAO templates with pore channels are fabricated by the well-known, two-step anodization.[17] The difference is the time of the 2nd step of anodization, we found that the anodization rate is about 80 nm min^{-1}, thus it is desirable to carry out the second anodization for 8 min to obtain about 800 nm thickness of channel height. Nevertheless, AAO templates with tapered pore channels are fabricated by the shape-controlled anodization. The shape-controlled anodization is that the shape of the pores in the AAO can be controlled by a process composed of a series of anodization and subsequent chemical etching treatments, most parts of which are performed under the same conditions as the two-step anodization except for the shape-controlled anodization. Briefly, the shape-controlled anodization is performed after removing the prepared irregular AAO film by the mixed solution with 2 wt% chromic acid and 5 wt% phosphoric acid. The second anodization process was performed at 0 °C for 2 min, and then at 35 °C for 5 min to widen holes in the 5 wt% phosphoric acid. The combined processes of 2 min anodization and 5 min hole-widening are repeated 5 times alternately. The tapered AAO templates with thickness of 800 nm are obtained. The schematic diagram of the process of fabrication is shown in Fig. 1.

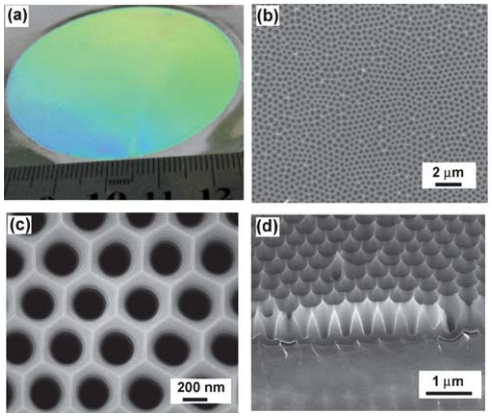

Fig. 1 (a) Two inch-large AAO template; (b) Top view of the SEM image of AAO with highly ordered hexagonal pore arrays; (c) The enlarged image confirming the hexagonal alignment of highly-ordered hole arrays; (d) Cross-sectional view of tapered pore arrays obtained through 5 times repetition of the anodization process and chemical etching treatments.

Formation of highly ordered epoxy cylindrical and conical pillar arrays

Firstly, the epoxy element A and element B are mixed adequately, and then the glue-state epoxy mixture is heated under fixed conditions of 80 °C and at the air pressure of 0.05 MPa for 30 min to obtain liquid epoxy resin. The epoxy mixture is spin-coated on the AAO template at 1000 rpm for 1 min. Subsequently, the AAO template is placed at 80 °C and 0.05 MPa air pressure for 10 min and then at 120 °C for 60 min to solidify the resin. The separation of the epoxy/AAO (epoxy layer on the top surface of AAO template) layer from the Al foil is achieved by selective wet chemical etching with a mixture of 0.1 M $CuCl_2$ and 10 wt% HCl solution (v/v). After separation, the epoxy/AAO layer is placed in 2 M NaOH solution for 15 min to remove the AAO membrane. Thus, the highly ordered epoxy nanostructured arrays are obtained.

Characterization methods

We firstly prepare a cylindrical glass mold with 6 cm inner diameter and 1.5 cm height. The planar AAO template 0.5 cm × 0.5 cm in size is stuck to the center of a glass slice with a length of 6 cm and height of 2 cm. Then the glass slice is positioned straight in the center of the glass mold. The liquid epoxy resin was injected into the glass mold. The transparent hemi-cylindrical epoxy sample was formatted after the resin was solidified adequately at 120 °C. Finally, the epoxy sample with the nano-strucutred arrays was obtained by removing the Al foil and AAO membrane using the approach mentioned above. We placed the epoxy sample at the center of the rotation stage. A laser beam with variable incident angle θ passes through the circular-edge of the epoxy to the center of the nanostructured arrays. A silicon detector located behind the nanostructured arrays can acquire the total light transmission. Thus, the angular-resolved transmission was acquired.

The light output measurements of the GaN based flip-chip LED were carried out in an integrating sphere system. Field

emission scanning electron microscopy (Nova NanoSEM 430) has been employed for the structural characterization of the AAO template and epoxy nanostructured arrays.

3 Results and discussion

3.1 Fabrication of highly ordered conical pillar arrays

To obtain the highly ordered conical pillar arrays experimentally on an epoxy surface, we have prepared the AAO template with well-ordered tapered pore arrays by the method of shape-controlled anodization of Al foils. The fabrication process is schematically depicted in Scheme 1. Firstly, highly ordered cylindrical pore arrays with a pitch of about 460 nm are fabricated by the conventional two-step anodization in the electrolyte of 1 wt% H_3PO_4 at constant applied voltage of 195 V and temperature of 0 °C.[24,27] Since the pitch of the pore arrays is determined by the applied voltage, we can control the diameter and depth of pores by adjusting the process parameters of time and temperature during anodization and chemical etching treatment. Then, the processes composed of a series of anodization and chemical etching treatments are alternately repeated 5 times to obtain tapered pore arrays. Thus, the tapered pore arrays have been obtained by optimizing the processes.

Fig. 1a shows the two-inch large AAO template. It presents a colour diffraction phenomenon due to the wavelength scale of about 460 nm which satisfies the Bragg diffraction condition to extract trapped optical modes significantly.[15] Fig. 1b shows the top-view scanning electron microscopy (SEM) image of the tapered pore arrays. The pattern shows well-aligned and hexagonally packed pore arrays with a mean pitch of 460 nm. The enlarged image (Fig. 1c) further confirms the wavelength-scale dimension and highly-ordered hexagonal alignment which is similar to 2D-PhC structures. Fig. 1d displays a cross-section view of the tapered pores arrays. The shape-controlled process consists of 5 times repetition of anodization and chemical etching treatments, the overall pore depth of about 800 nm is determined by the total anodization time. Note that the maximum diameter of pores is almost 460 nm, thus the tip angle is about 32°. Highly ordered tapered pore arrays considered as a special 2D-PhC are a promising functional material for high optical performance.

The hot embossing technique is employed to fabricate highly ordered epoxy conical pillar arrays using the AAO template. The epoxy resin is heated to 80 °C where its viscosity can be greatly reduced. After the epoxy resin is spin-coated onto the AAO surface, the epoxy/AAO template is then placed into the vacuum-assisted oven at the fixed temperature of 80 °C for 10 min to let the epoxy resin infiltrate the pores adequately. At last, we bake the sample at 120 °C for one hour to solidify the epoxy resin. After removal of the residual Al layer and AAO membrane layer by chemical treatments, the epoxy conical pillar arrays are obtained. For reference, the cylindrical pillar arrays with about 460 nm pitch and 800 nm depth on the epoxy surface have also been fabricated using conventional two-step anodization followed by hot embossing.

Fig. 2a shows the replica mold of a two inch area of epoxy conical pillar arrays. The uniform blue pattern corresponds to the array's pitch of about 460 nm. The inset of airy diffraction pattern is formed under the normal incident direction of white light beam from the object lens of the microscope. Airy rings suggest that the highly ordered arrays are rather uniform but not perfectly hexagonally aligned due to the AAO's natural domain property.[28] It is remarkable to note that the replica mold is suitable to be the template of nanoimprint lithography (NIL). Fig. 2b–2c displays the top and cross-sectional view of SEM images of the arrays. Carefully inspecting the SEM images, some

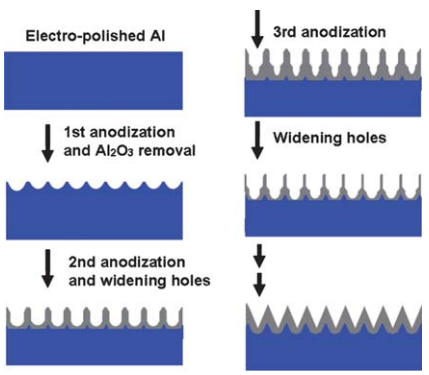

Scheme 1 Procedure for the fabrication of tapered pore arrays.

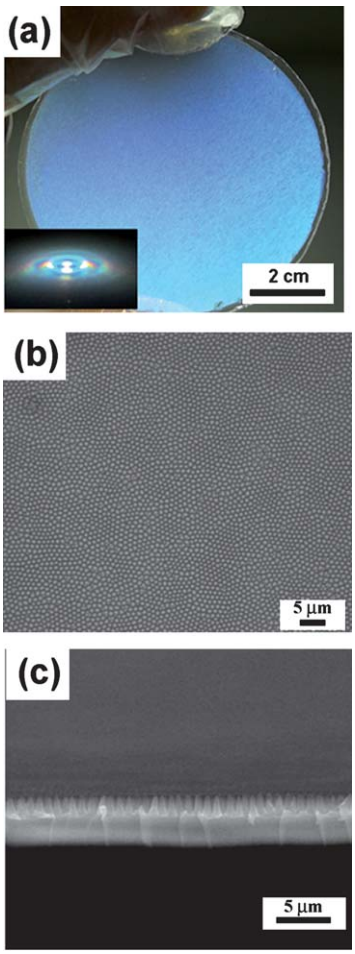

Fig. 2 (a) Epoxy replica mold from the AAO template, the inset is the airy diffraction pattern formed by white light beam incidence from the objective lens of the microscope; (b) the top view of the conical pillar arrays; (c) the cross-sectional view of the conical pillar arrays.

imperfect arrays exist in the SEM images due to the electron beam scanning damage. The cross-sectional view shows the nanostructures have a conical morphology. The height, the base diameter and the top angle of the conical pillars are about 800 nm, 460 nm and 32°, respectively, which are consistent with those of the tapered pores. Hence it has been proved that the epoxy resin is an excellent polymer material to transfer nanostructured arrays from the AAO templates. Moreover, the aspect ratio of about 1.7 is an appropriate parameter for ensuring most of conical pillars are standing up straight on the epoxy surface. Due to the shape-controlled anodization, the diameter of the conical pillars is continually reduced from the bottom to the surface which induces a filling factor of epoxy increasing gradually, and so the refraction index of the array layer varies continually from 1.56 (the refraction index of epoxy) to 1 (the refraction index of air) with a slope of 3.5. In other words, the conical pillar arrays could be also considered as a film with a graded-refractive-index from the bulk substrate to air.

3.2 Optical transmission properties

To investigate the optical transmission properties of the nanostructured arrays, we have adopted a convenient approach of inspecting the cone or cylinder arrays on a special configuration of a transparent hemi-cylindrical epoxy sample similar to our previous reports.[13,29] The cone and cylinder arrays are transferred to the flat center of the specially designed transparent epoxy hemi-cylinder. In this way, we could then directly observe and measure the diffracted transmission depending on the incident light from the medium to air. The critical angle of epoxy is $\theta_{crit} = 40°$, determined by the refractive index of 1.56.

During measurement, the hemi-cylindrical epoxy sample is placed at the center of the rotational stage. A laser beam with variable incident angle θ passes through the circular-edge of the epoxy and impinges towards the center of the arrays by an angle resolution of 2°. A silicon detector located behind the array acquires the total light transmission through epoxy/arrays. Fig. 3a and 3b exhibit a sharp contrast between the planar epoxy and cone array patterned epoxy samples impinged by an incident beam from a 532 nm green laser at the same incident angle of 50°, which is larger than the critical angle of θ_{crit}. Obviously, it illustrates TIR occurring on the planar epoxy sample as shown in Fig. 3a. No less than our expectation from Fig. 3b, most of the light is still transmitted into the air on the cone arrays sample. Although there is still a part of the light reflected due to the 2D-PhC diffraction effect, the diffracted transmission is dominant above the critical angle.

We have also measured the incident angular-resolved light transmission of the epoxy conical pillar arrays. Moreover, as a comparative study, the incident angular-resolved light transmission of epoxy cylindrical pillar arrays and planar epoxy has also been measured, as shown in Fig. 4.

It is reasonable to regard the cylindrical pillar arrays as a 2D-PhC for its highly ordered alignment and wavelength-scale pitch, and the conical pillar arrays are believed to be special 2D-PhCs composed of multilayer 2D-PhCs with the filling factor gradually increasing from the bottom towards the surface. The unique diffraction mechanism of the special 2D-PhCs can contribute to the high transmission. Below the critical angle region, the light transmission of 2D-PhCs decreases as some of the originally extracted modes are coupled to the reciprocal lattice of 2D-PhCs and turned back to trapped guided modes.[13,14] However, the light transmission of the special 2D-PhCs is slightly higher than that of the planar epoxy sample. We attribute the enhancement to the special 2D-PhCs' graded filling factor which induces the reciprocal lattice of 2D-PhCs to change gradually, and results in trapped modes coupling with the reciprocal lattice and becoming extracted modes. When the incident angle is larger than the critical angle, all of the light is trapped into guided modes for the reference planar epoxy sample due to TIR. Nevertheless, extra higher light transmitted from the surface of conical pillar arrays has been obtained compared to that of the planar epoxy sample. The reciprocal lattice of 2D-PhCs not only couples guided modes to extracted modes but also couples the

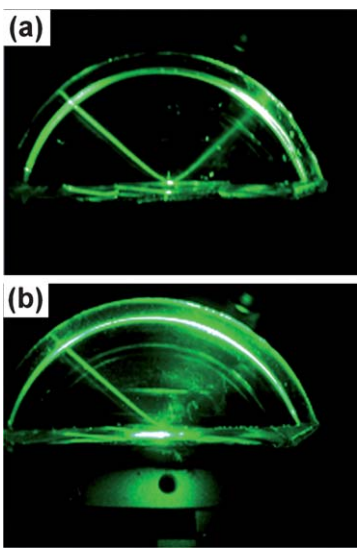

Fig. 3 Epoxy hemi-cylinders impinged by the incidence of 532 nm laser beam. (a) Total reflection occurring when the incident angle is 50° ($>\theta_{crit}$) for the planar epoxy sample; (b) Epoxy conical pillar arrays reducing the occurrence of total reflection.

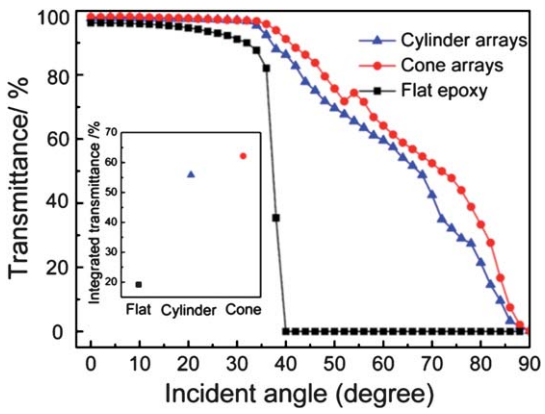

Fig. 4 Experimental transmission efficiency curves for planar epoxy, cylinder and cone arrays patterned epoxy, respectively. Shown in the inset is the integrated transmission of the different kinds of nanostructure arrays and the reference.

extracted modes back to guided modes again.[16,17] Therefore, the light extraction enhancement of 2D-PhCs is limited. However, for special 2D-PhCs, the diffraction mechanism of the reciprocal lattice coupling trapped guided modes into extracted modes is dominant due to the graded-changing reciprocal lattice. Consequently, higher light transmission is obtained. Moreover, we have also obtained the total transmission of the integrated data

$$T = \int_0^{2\pi} d\theta \int_0^{\pi/2} T(\theta, \phi) \sin\theta d\phi \quad (1)$$

over the whole incident angle θ and azimuth angle ϕ from the formula (1). As shown in the inset of Fig. 4, the integrated transmission of planar epoxy, cylindrical pillar and conical pillar arrays is 19.2%, 55.8% and 62.2%, respectively. Thus, the integrated transmission of conical pillar arrays is confirmed to be 223% and 11.3% higher than that of planar epoxy and the cylindrical pillar arrays. The remarkable enhancement is attributed to the unique diffraction effect of the cone arrays.

It is found that the cylindrical pillar arrays extract almost 56% of light transmission, which is much higher than that of conventional 2D-PhCs and slightly lower than that of conical pillar arrays. Therefore, it is necessary to investigate the shape of cylinder arrays carefully. As shown in Fig. 5a, the top-surface of cylindrical pillars is not planar circles but hemi-spheres which act as a nanolens or graded-refractive-index layer. The graded-refractive-index layer induces the change of 2D-PhCs' filling factor, and hence results in the reciprocal lattice changing gradually. Consequently, the higher light transmission is obtained due to the graded reciprocal lattice's function to extract guided modes to escape into the air. Fig. 5b shows the corresponding shape of conical pillar arrays. We intentionally created an AAO template with tapered pore arrays to obtain conical pillar arrays with a gradually changing refractive index. Although the parameters of conical pillar arrays still need to be optimized, their better transmission property is demonstrated compared to that of cylindrical pillar arrays.

3.3 Application in improving light extraction of GaN-based flip-chip LED

The cylindrical pillar arrays, especially the conical pillar arrays, have an important potential application in improving the light extraction efficiency of GaN-based blue LEDs due to their excellent transmission properties. To directly demonstrate their use in enhancing light extraction of GaN-based LEDs, we proposed a novel package configuration on a GaN-based flip-chip LED (FC LED) with a size of 1 mm × 1 mm and an emission wavelength of about 460 nm. The hot embossing technique is employed to form a series of nanostructured arrays on the topmost encapsulated epoxy above the sapphire substrates of FC LED using an AAO template. Scheme 2 shows the schematic diagram of the package configuration. The procedures of the hot embossing on the encapsulation of FC LED, the steps of which are most similar to the formation of epoxy cone arrays, are very simple and reliable. The additional step to press the sapphire substrate of FC-LED to liquid epoxy resin is carried out at a pressure of about 5×10^5 Pa after the step of spin-coating liquid epoxy resin onto the AAO template. The light output power and light far field distribution measurements are carried out in an integrating sphere system assembled with a fiber spectrometer. FC LED with planar epoxy, epoxy cylinder and cone arrays were tested and compared.

Fig. 6a shows the typical curves of light output power *versus* forward current (L–I) in the FC LED. Obviously, the power output increases significantly in both nanostructured array encapsulated LEDs. Moreover, owing to the diffraction effect, the encapsulated LED with cone arrays displays the highest light output power. At an injection current of 350 mA, the cone array and cylinder array LEDs were enhanced by 46.8% and 34.9%, respectively. Fig. 6b exhibits the typical far-field emission profiles of epoxy encapsulated LEDs with and without nanostructured arrays measured at the driving current of 350 mA. Noticeably, both encapsulated LEDs with nanostructured arrays have higher emission intensities compared to that of the planar sample. Moreover, the light enhancement focuses on the surface normal view angle of ±30°. As expected, the light output of the cone array encapsulated sample is slightly higher than that of the cylinder array encapsulated sample.

Both the results of L–I characteristics and far-field emission profiles are in good agreement with the optical transmission properties of each nanostructure array. The excellent diffraction effect plays an important role in improvement of light extraction of both conical pillar array and cylindrical pillar array patterned FC LEDs. The relatively small difference of light extraction enhancement between two kinds of nanostructure array patterned FC LED is mostly attributed to the tip of cylindrical pillars being not planar circles but instead hemispherical nanolen, which acts as a graded-refractive-index layer and is beneficial for light escaping to the air. The parameters of conical pillar arrays, such as the aspect ratio and the top angle, also need to be optimized to obtain larger light extraction. It is worthy of note that the enhancement factor of light extraction is still limited so far since the light emitting to the sapphire substrate and epoxy is limited. If the cone arrays layer is closer to the active layer where most guided light converges, the maximal improvement of light extraction efficiency will be obtained. Further work is currently in progress.

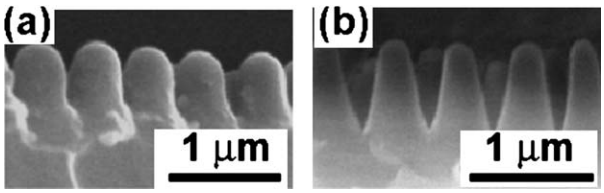

Fig. 5 Cross-sectional views of SEM images for (a) cylindrical pillar arrays and (b) conical pillar arrays.

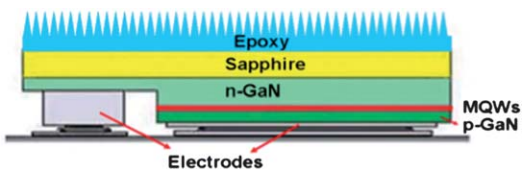

Scheme 2 Schematic diagram of the thin epoxy encapsulated GaN based FC LED with conical pillar array.

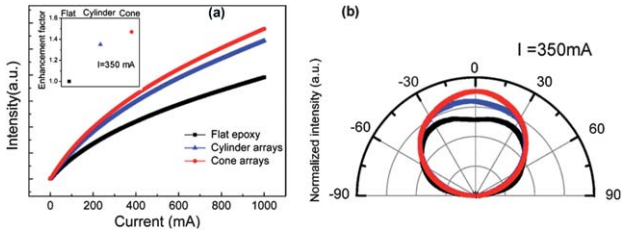

Fig. 6 (a) L–I curves for the thin epoxy encapsulated GaN based FC-LEDs with cone arrays, cylinder arrays surface and planar surface; (b) The corresponding far-field emission profile for the LEDs mentioned above at the injection current of 350 mA.

4 Conclusions

We have reported a facile and cost-effective approach for the formation of wavelength-scale conical pillar arrays on a large surface area of epoxy. The highly ordered epoxy cone arrays with a pitch of about 460 nm and a height of about 800 nm were successfully fabricated by the technique of shape-controlled anodization of Al foil followed by hot embossing. The integrated transmission of conical pillar arrays was confirmed to be 223% and 11.3% higher than that of planar epoxy and the cylindrical pillar arrays, respectively. We attribute the light transmission enhancement to the diffraction effect of the 2D-PhC multilayer with gradually reducing fill-factor towards the surface. The light output power of the epoxy encapsulated GaN-based FC LED with cone and cylinder arrays compared to that of the planar epoxy encapsulated sample is improved by 46.8% and 34.9%, respectively. We hope that this work will open a new way for the application of AAO in photonics and other fields.

Acknowledgements

The authors gratefully acknowledge Dr T. Dai and Dr K. Bao for the previous contributions on AAO fabrication and hot embossing technique. This work was supported by National Key Basic Research Special Foundation of China under Grant No. TG2011CB301905, TG2007CB307004, TG2011CB301904, and Science and Technology Project of Beijing under Grant No. Z101103050410003, and Natural Science Foundation of China under Grant Nos. 61076012, 60876063, 60676032.

Notes and references

1 E. F. Schubert and J. K. Kim, *Science*, 2005, **308**, 1274.
2 J. K. Kim, S. Chhajed, M. F. Schubert, E. F. Schubert, A. J. Fischer, M. H. Crawford, J. Cho, H. Kim and C. Sone, *Adv. Mater.*, 2008, **20**, 801.
3 E. F. Schubert. *Light Emitting Diodes*; Cambridge University Press: Cambridge, U.K., 2006.
4 J. J. Wierer, A. David and M. M. Mischa, *Nat. Photonics*, 2009, **3**, 163–169.
5 C. Wiesmann, K. Bergenek, N. Linder and U. T. Schwarz, *Laser & Photon. Rev.*, 2008, 1.
6 Y. M. Song, E. S. Choi, J. S. Yu and Y. T. Lee, *Opt. Express*, 2009, **17**, 20991.
7 K. Saxena, V. K. Jain and D. S. Mehta, *Opt. Mater.*, 2009, **32**, 221.
8 K. Saxena, D. S. Mehta, V. K. Rai, R. Srivastava, G. Chauhan and M. N. Kamalasanan, *J. Lumin.*, 2008, **128**, 525.
9 Y. F. Li, F. Li, J. H. Zhang, C. L. Wang, S. J. Zhu, H. J. Yu, Z. H. Wang and B. Yang, *Appl. Phys. Lett.*, 2010, **96**, 153305.
10 C. F. Lai, C. H. Chao, H. C. Kuo, H. H. Yen, C. E. Lee and W. Y. Yeh, *Appl. Phys. Lett.*, 2009, **94**, 123106.
11 D. H. Kim, C. O. Cho, Y. G. Roh, H. Jeon, Y. S. Park, J. Cho, J. S. Im, C. Sone, Y. Park, W. J. Choi and Q. H. Park, *Appl. Phys. Lett.*, 2005, **87**, 203508.
12 T. Dai, B. Zhang, Z. S. Zhang, D. Liu, X. Wang, K. Bao, X. N. Kang, J. Xu and X. Zhu, *Chin. Phys. Lett.*, 2007, **24**, 979.
13 C. Xiong, B. Zhang, X. N. Kang, T. Dai and G. Y. Zhang, *Opt. Express*, 2009, **17**, 23684.
14 C. Xiong, B. Zhang, X. N. Kang, X. X. Fu and G. Y. Zhang, *Sci. China, Ser. E: Technol. Sci.*, 2011, **54**, 23.
15 X. X. Fu, B. Zhang, X. N. Kang, C. Xiong and G. Y. Zhang, *Sci. China, Ser. E: Technol. Sci.*, 2011, **54**, 1.
16 T. Yanagishita, K. Nishio and H. Masuda, *Appl. Phys. Express*, 2008, **1**, 012002.
17 H. Masuda, H. Yamada, M. Satoh, H. Asoh, M. Nakao and T. Tamamura, *Appl. Phys. Lett.*, 1997, **71**, 2770.
18 A. P. Li, F. Muller, A. Birner, K. Nielsch, U. Gosele and J. Appl, *Phys.*, 1998, **84**, 6023.
19 J. K. Kim, A. N. Noemaun, F. W. Mont, D. Meyaard, E. F. Schubert, D. J. Poxson, H. Kim, C. Sone and Y. Park, *Appl. Phys. Lett.*, 2008, **93**, 221111.
20 P. B. Clapham and M. C. Hutley, *Nature*, 1973, **244**, 281.
21 B. Paivanranta, T. Saastamoinen and M. Kuittinen, *Nanotechnology*, 2009, **20**, 375301.
22 T. Yanagishita, K. Nishio and H. Masuda, *Appl. Phys. Express*, 2008, **1**, 067004.
23 T. Yanagishita, K. Nishio and H. Masuda, *Appl. Phys. Express*, 2009, **2**, 022001.
24 T. Yanagishita, K. Yasui, T. Kondo, Y. Kawamoto, K. Nishio and H. Masuda, *Chem. Lett.*, 2007, **36**, 530.
25 K. Choi, S. H. Park, Y. M. Song, Y. T. Lee, C. K. Hwangbo, H. Yang and H. S. Lee, *Adv. Mater.*, 2010, **22**, 3713.
26 H. Ichikawa and T. Baba, *Appl. Phys. Lett.*, 2004, **84**, 457.
27 D. S. Kim, H. S. Lee, J. Lee, S. Kim, K. H. Lee, W. Moon and T. H. Kwon, *Microsyst. Technol.*, 2007, **13**, 601.
28 K. Nielsch, J. Choi, K. Schwirn, R. B. Wehrspohn and U. Gosele, *Nano Lett.*, 2002, **2**, 677.
29 C. Xiong, B. Zhang, X. N. Kang, T. Dai and G. Y. Zhang, *Semicond. Sci. Technol.*, 2010, **25**, 065006.